

#### Contents lists available at ScienceDirect

#### Physica B

journal homepage: www.elsevier.com/locate/physb



## Effect of Al substitution on the structural and magnetic properties of Co-Zn ferrites



N. Murali<sup>a,b,\*</sup>, S.J. Margarette<sup>b</sup>, G. Pavan Kumar<sup>a</sup>, B. Sailaja<sup>a</sup>, S. Yonatan Mulushoa<sup>b</sup>, P. Himakar<sup>b</sup>, B. Kishore Babu<sup>c</sup>, V. Veeraiah<sup>b</sup>

- <sup>a</sup> Advanced Analytical Laboratory, DST-PURSE Programme, Andhra University, India
- <sup>b</sup> Department of Physics, Andhra University, Visakhapatnam, Andhra Pradesh, India
- <sup>c</sup> Department of Engineering Chemistry, AUCE(A), Andhra University, Visakhapatnam 530003, Andhra Pradesh, India

#### ARTICLE INFO

# Keywords: Co-Zn-Al ferrite XRD SEM FT-IR Saturation magnetization Coercivity

#### ABSTRACT

In this work we investigate the effect of aluminum (Al) substitution on the structural, morphological and magnetic properties of  $\mathrm{Co}_{0.5}\mathrm{Zn}_{0.5}\mathrm{Al}_x\mathrm{Fe}_{2-x}\mathrm{O}_4$  (x = 0.0, 0.05 and 0.1) prepared by sol-gel method. The structural and magnetic properties are performed by using X-ray powder diffraction (XRD), scanning electron microscope (SEM), Fourier transform infrared spectra (FT-IR) and Vibrating Sample Magnetometer (VSM) studies. The XRD data revealed the formation of single phase cubic spinel with crystallite sizes around 45.83–51.84 nm for Al substituted samples. Two significant absorption bands around 600 and 400 cm<sup>-1</sup> are observed from FT-IR spectra of the samples under investigation, which confirmed the formation of a single-phase cubic spinel. Interionic bond lengths and bond angles confirm the solubility of Al in the spinel lattice and support the observed variation in magnetic properties. Using a vibrating sample magnetometer (VSM), saturation magnetization and coercivity are measured. A decrease in lattice parameter and saturation magnetization with increasing Al concentration is attributed to the difference in the ionic radii and weakening of exchange interactions.

#### 1. Introduction

Magnetic photo-catalyst has attracted increasing attention because it can overcome the limitation of separation from the liquid phase because of iron oxide bond present in their nanostructure [1-5]. Therefore, it is important to find a strategy for making these photocatalysts to posses' magnetism. The magnetism of spinel nanoferrites is derived from super exchange between cations in tetrahedral (A-site) and octahedral (B-site) including A-B exchange, B-B exchange and A-A exchange. Therefore, the magnetic properties of spinel is related to the distribution species of cations in A-site and B-site. They reported that A-B super-exchange interaction decreases due to the addition of doped ions which preferentially occupy the octahedral B-sites. Spinel nano-ferrites have thus been used in enormous technological applications, including magnetic recording, drug delivery, catalysts, sensors, microwave absorption, ferro-fluids, information storage systems and magnetic resonance imaging [6–8]. Several preparation methods have been used to prepare spinel nano-ferrites including coprecipitation, hydrothermal, sol-gel auto combustion, and microwave combustion [9–13]. Among these methods, the citrate precursor method is advantageous because of the homogeneous mixing of the cations at the molecular level, the stoichiometric control efficiency, the limited size distributions and the lower-temperature phase formation. Many authors studied about the effect of trivalent ions substitution in B-site on the magnetic and electrical properties of different ferrites. Synthesized nanoparticles of  $Cr_xCo_{0.5-x}Zn_{0.5}Fe_2O_4$ , by systematically replacing of Co with Cr in  $Co_{0.5}Zn_{0.5}Fe_2O_4$ , reported the effect of Cr substitution on structural and magnetic properties of the above series. They also studied the structural and magnetic properties of Cr doped  $Ni_{0.5}Zn_{0.5}Fe_{2.x}Cr_xO_4$  nano-powders [14,15].

In this work, we have examined systematically the structural and magnetic properties of  $\text{Co}_{0.5}\text{Zn}_{0.5}\text{Fe}_{2\text{-x}}\text{Al}_x\text{O}_4$  (x = 0.0, 0.05 and 0.1) materials and the effects of simultaneous substitution of  $\text{Zn}^{2\text{+}}$  and  $\text{Al}^{3\text{+}}$  ions on the magnetic properties of cobalt ferrites.

#### 2. Results and discussion

Preparation of  $Co_{0.5}Zn_{0.5}Al_xFe_{2-x}O_4$  (x = 0.0, 0.05 and 0.1) ferrites has been done by the sol-gel method. The AR grade  $Fe(NO_3)_3 \cdot 9H_2O$ ,  $Co(NO_3)_2 \cdot 6H_2O$ ,  $Al(NO_3)_3 \cdot 9H_2O$ ,  $Zn(NO_3)_2 \cdot 6H_2O$  and citric acid are

<sup>\*</sup> Corresponding author at: Advanced Analytical Laboratory, DST-PURSE Programme, Andhra University, India. E-mail address: muraliphdau@gmail.com (N. Murali).

N. Murali et al. Physica B 522 (2017) 1–6

weighed in desired stoichiometric proportions and are dissolved in the minimum amount of distilled water. The individual solutions are then mixed together and the pH value is adjusted to 5-7 by adding NH<sub>4</sub>OH solution. The solution is then burnt to self ignition to obtain a loose powder. The powders are annealed to  $1000~^{\circ}\text{C}$  in a muffle furnace for 2~h.

The powder X-ray diffraction (XRD) data of the samples has been collected on a Rigaku CuK $\alpha$  diffractometer with diffraction angles of 20° to 80° in increments of 0.02°. The unit cell lattice parameter is obtained by the least square fitting method from the d-spacing and (h k l) values. Further, the crystallite size of the sample is obtained from XRD pattern by applying Scherrer's equation. The particle morphology of the powder is observed using a field effect scanning electron microscopy image taken from Carl Zeiss, EVOMA 15, Oxford Instruments, Inca Penta FETx3. JPG. The Fourier transform infrared spectra are recorded using Nicolet 6700 and followed by the KBr pressed pellet technique to determine the structures of the calcined ferrite materials. The magnetic properties have been measured at room temperature by a Vibrating Sample Magnetometer (VSM) (155, PAR) upto a magnetic field of  $\pm$  10 kOe.

#### 3. X-ray diffraction studies

The X-ray diffraction (XRD) patterns of  $\text{Co}_{0.5}\text{Zn}_{0.5}\text{Al}_x\text{Fe}_{2-x}\text{O}_4$  (x = 0.0, 0.05 and 0.1) powders sintered at 1000 °C / 2 h are shown in Fig. 1. The formation of spinel ferrite phase is confirmed with JCPDS file no. 08–0234 from the intense X-ray diffraction lines corresponding to (220) (311) (222) (400) (422) (511) (440) planes using the standard diffraction plots [16]. There is a decrease in the lattice parameter as showen in Table 1, with Al³+ ion substitution which is ascribed to the ionic radius difference between the substituted Al³+ (0.051 nm) and the displaced Fe³+ (0.064 nm) ions which is in accordance with Vegard's law [17]. The variation of lattice constant with Al³+ substitution inevitably supports the occupancy of the Al ions into the host Co-Zn ferrite lattice.

The lattice parameters are calculated to be 8.3911–8.3661 Å for  $Co_{0.5}Zn_{0.5}Al_xFe_{2-x}O_4$  (x = 0.0, 0.05 and 0.1), respectively. The lattice parameter decreases with the substitution of  $Zn^{2+}$  ions with  $Co^{2+}$  ions, to accommodate the  $Zn^{2+}$  ion of relatively larger ionic radii (88 p.m.) as compared to that of  $Co^{2+}$  ion (83.8 p.m.) [20]. With further substitution of  $Fe^{3+}$  ions with  $Al^{3+}$  ions, the lattice parameter decreased attributing to the smaller ionic radii of  $Al^{3+}$  ion as compared to  $Fe^{3+}$  ion shown in Table 1. The peaks in the XRD patterns are broad, which may be due to small particle size.

The unit cell lattice parameter is obtained by the unit cell software from the  $2\theta$  and (hkl) values. The crystallite size of magnesium ferrite

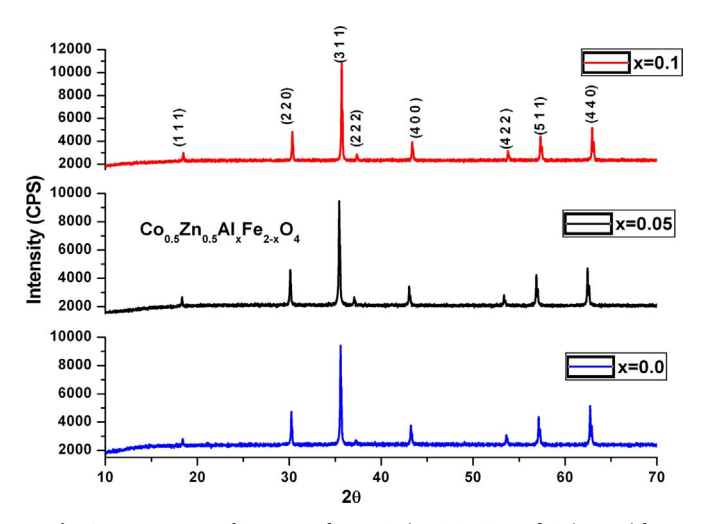


Fig. 1. XRD patterns of  $Co_{0.5}Zn_{0.5}Al_xFe_{2-x}O_4$  (x = 0.0, 0.05 and 0.1) materials.

Table 1 Lattice parameter, unit cell volume and crystallite size of  $Co_{0.5}Zn_{0.5}Al_xFe_{2-x}O_4$  (x = 0.0, 0.05 and 0.1) materials.

Compound	a (Å)	Unit cell Volume V (Å) <sup>3</sup>	Crystallite size (nm)
$\text{Co}_{0.5}\text{Zn}_{0.5}\text{Fe}_2\text{O}_4$	8.3911	590.8167	45.83
$Co_{0.5}Zn_{0.5}Al_{0.05}Fe_{1.95}O_4$	8.3405	580.1944	51.84
$Co_{0.5}Zn_{0.5}Al_{0.1}Fe_{1.9}O_4$	8.3661	585.5642	48.79
$Co_{0.5}Zn_{0.5}Fe_2O_4$ [18]	8.418	596.52	67.10
$Co_{0.5}Zn_{0.5}Fe_2O_4$ [19]	8.41	-	
$Co_{0.5}Zn_{0.5}Al_{0.2}Fe_{1.8}O_4$ [19]	8.37	_	-

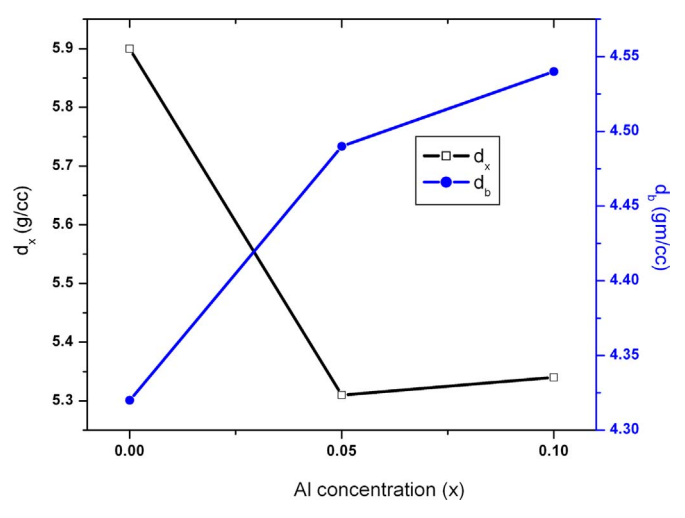


Fig. 2. X-ray and bulk density of  $Co_{0.5}Zn_{0.5}Al_xFe_{2-x}O_4$  (x = 0.0, 0.05 and 0.1) materials.

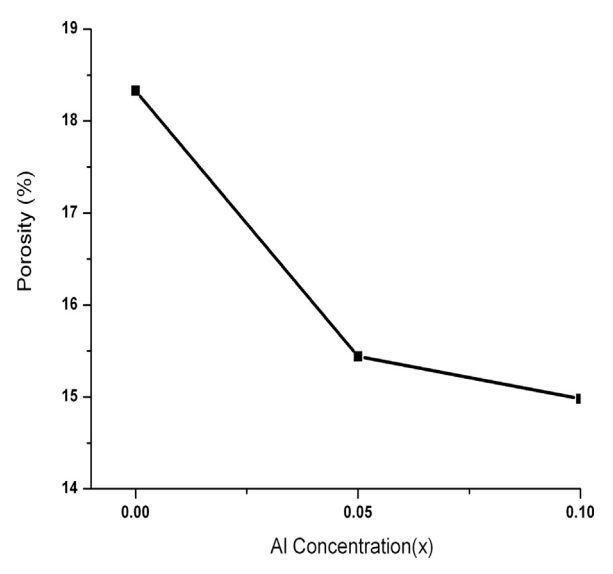


Fig. 3. Porosity of  $Co_{0.5}Zn_{0.5}Al_xFe_{2-x}O_4$  (x = 0.0, 0.05 and 0.1) materials.

present is investigated based on X-ray diffraction line broadening and calculated using Scherrer equation [21].

$$D = \frac{K\lambda}{\beta \cos \theta}$$

where D is the average crystalline size,  $\beta$  is the Full Width at Half Maximum of the line broadening of the maximum reflection in radians,  $\theta$  is the angle corresponding to the peak position,  $\lambda$  is the wavelength of X-ray radiation equal to 1.542 Å, K is the Shape factor of average crystallite  $\sim$  0.9.

The average lattice constant value (a) is obtained using  $2\theta$  values of the most intense peaks using Bragg's diffraction [22] condition, given

#### Download English Version:

### https://daneshyari.com/en/article/5491757

Download Persian Version:

https://daneshyari.com/article/5491757

<u>Daneshyari.com</u>